

## Shaking-induced stress anisotropy in the memory effect of paste

SO KITSUNEZAKI<sup>1</sup>, AKIO NAKAHARA<sup>2</sup> and YOUSUKE MATSUO<sup>2</sup>

<sup>1</sup> *Research Group of Physics, Division of Natural Sciences, Faculty of Nara Women's University - Nara 630-8506, Japan*

<sup>2</sup> *Laboratory of Physics, College of Science and Technology, Nihon University - Funabashi, Chiba 274-8501, Japan*

PACS 46.50.+a – Fracture mechanics, fatigue and cracks  
PACS 46.35.+z – Viscoelasticity, plasticity, viscoplasticity  
PACS 83.80.Hj – Suspensions, dispersions, pastes, slurries, colloids

**Abstract** – When paste of fine granular particles and water is shaken in one direction and then left undisturbed, memory of the direction of shaking is retained for a sufficiently long time to result in a directional crack pattern that appears after drying. Although it has been conjectured that anisotropy in residual stresses caused by plastic deformation is responsible for this memory effect, to this time, no evidence of such anisotropy has been found. We experimentally investigated the stress in drying paste by measuring the bending of elastic plates supporting the paste sample and found stress anisotropy developing in paste. Additional bending tests suggested that paste retains plasticity during the drying process and that plastic deformation is not always frozen in place after initial shaking.

---

**Introduction.** – Paste-like mixtures of fine granular materials and liquid, such as clay powder and water, retain memory of the anisotropy of mechanical perturbations, and this can lead to the formation of directional crack patterns as the paste dries. It has been found that this memory effect has various types, which are determined by the properties of the granular material, the liquid content of the initial state, and the manner in which the perturbation is applied, for example, through mechanical shaking, forced flow in the paste, application of electric or magnetic fields, etc [1–7]. The memory effect in the case of horizontal oscillation (*memory effect of shaking*) is particularly common in pastes and has been thoroughly investigated. Memory of shaking is created when paste with plasticity experiences shear stresses larger than the yield stress. In the situation that a uniform sample of paste is prepared, shaken for a short time along one direction, and then left undisturbed to dry, eventually cracks aligned perpendicularly to the direction of shaking develop, and subsequently cracks parallel to this direction appear in a ladder form. Phenomenological elastoplastic theories have been proposed to describe memory of shaking, and it is generally believed that shaking creates anisotropy in the residual stresses, and this anisotropy determines the direction of cracking [8–10].

To this time, the investigation of desiccation cracks has been the only method used to detect anisotropy induced

by shaking. For this reason, it has not been possible to test the residual stress theories and to clarify how the initial anisotropy induced in a paste affects crack formation. Residual stresses are generally less than the yield stress. When shaking is applied to a paste, it behaves like a liquid, and the yield stress is at most of the order of 10Pa. Contrastingly, when a layer of paste is dried uniformly in a container with a hard flat bottom, the hydrostatic pressure of fluid contained in pores decreases, and as a result, the internal stresses of the order of 10<sup>4</sup>Pa appear up to crack formation [11,12]. With this great difference between the yield stress in the paste at the initial time and the internal stress required for cracking, if there exists some anisotropy in residual stresses initially, significant amplification of this anisotropy should be necessary to control the direction of crack formation.

We experimentally investigated horizontal stresses appearing during the drying process of a paste sample. This study started with the discovery of a simple phenomenon: We found that when a container with a thin elastic sheet acting as its bottom holds a uniform layer of paste, that is shaken horizontally in one direction before drying, the elastic bottom gradually bends up in the direction of the initial shaking as the paste dries until cracks form. This behavior is depicted in Fig. 1. If the paste sample is thin compared with the length and width of the container, the bending direction does not depend on the aspect ratio of

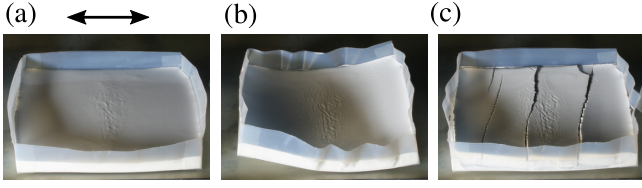


Fig. 1: Directional buckling of a thin elastic plate, caused by the memory effect of shaking in the layer of paste on it. A sample of  $\text{CaCO}_3$  paste with initial solid volume fraction  $\phi(0) = 0.48$  was poured into a container with a bottom plastic composed of polyvinyl chloride ( $100 \times 100 \times 0.5 \text{ mm}^3$ ) and soft walls made of a thin PTFE tape. (a) A horizontally oscillating mechanical perturbation of frequency 120 rpm and amplitude 15 mm was applied before drying for 5 min in the direction indicated by the arrow. (b) Subsequently, the plate bent along with the elastic bottom as it dried. (c) Finally, cracks perpendicular to the direction of shaking formed.

the bottom and is insensitive to the lateral boundary conditions [13]. Thus we can estimate the horizontal stresses in the bending direction on the basis of the curvature of the elastic bottom. The stress measurement of using the deflection of an elastic plate has been used in some researches for drying films [14,15]. For simultaneous measurement of horizontal stresses parallel and perpendicular to the direction of shaking, we constructed special containers to which four thin elastic plates (plate springs) were attached to the bottom in order to allow vertical displacement. Our measurements confirmed that stress anisotropy increases significantly during the drying process, up to crack formation. We also report the results of bending tests applied to a paste sample during the drying process.

**Experiments.** – We prepared a uniform sample of calcium carbonate ( $\text{CaCO}_3$ ) paste in the container with four stainless steel springs, as shown in Fig. 2(a), and then monitored the displacement of each spring and the total weight of the layer as this paste dried.

The four springs were fixed to the side of a square rigid metal plate with a  $100 \times 100 \text{ mm}^2$  face using 1 mm-thick clamping plates in order to make them flush with the face. Each spring covers a rectangular area of length  $L = 40 \text{ mm}$  and width  $W = 80 \text{ mm}$  on the bottom of the container and can bend only along the direction perpendicular to the fixed side. The opposite side is folded upward at a right angle to make a hard wall of height 10 mm, and the remaining walls are made of soft PTFE tape of thickness 0.16 mm. We used three types of containers with springs of thickness  $h = 0.15, 0.2$  and  $0.3 \text{ mm}$ , respectively.

Paste consisting of  $\text{CaCO}_3$  powder (JIS Z 8901 test powder 1-16) and ion-exchanged water was used in our experiments.  $\text{CaCO}_3$  particles are almost completely insoluble in water and have diameters of  $0 - 20 \mu\text{m}$ . The 50% over-size diameter based on mass is  $4.5 \mu\text{m}$ . A morphological phase diagram of crack patterns and its relation to the yield stress of paste were presented by Nakahara, Shinohara and Matsuo for this powder [3]. The paste exhibits

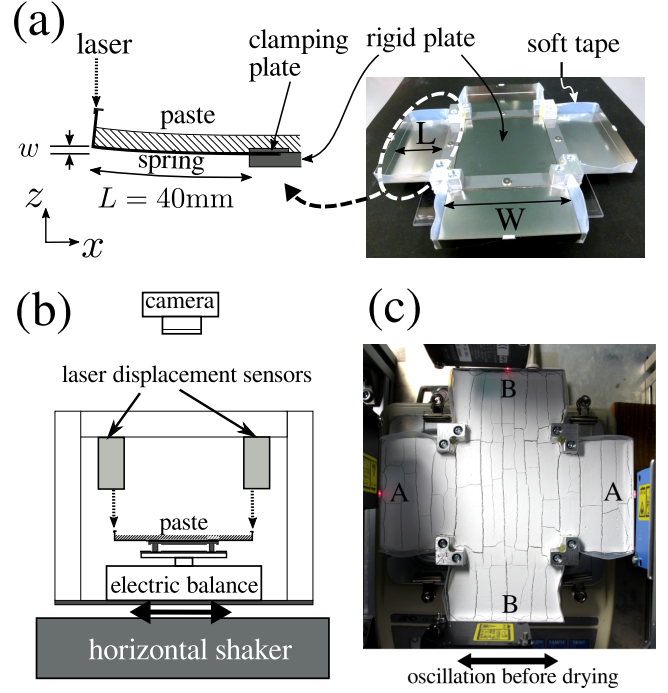


Fig. 2: (a) Photograph of a container and a schematic cross-section of a spring filled with paste. A tiny piece of plastic positioned at the top center of the hard wall acted as the target for a laser displacement sensor. (b) The side view of the experimental setup. (c) A top view of a typical crack pattern after drying. The springs labeled “A” and “B” bend up along different directions.

the memory effect when the initial solid volume fraction,  $\phi(0)$ , is between the liquid limit, 0.264, and the plastic limit, 0.520. In order to compare water-rich and water-poor conditions, we investigated two cases for the initial mass ratio,  $\text{CaCO}_3 : \text{H}_2\text{O} = 100 : 140$  (corresponding to  $\phi(0) = 0.207$ ) and  $100 : 58$  ( $\phi(0) = 0.387$ ). In the water-rich case, the paste cannot remember the direction of shaking, as  $\phi(0) = 0.207$  is less than the liquid limit. We dried samples without initial shaking. In the water-poor case, the paste can retain memory of shaking. We applied unidirectional horizontal oscillation to the paste for 5 min before substantial drying had taken place by using a horizontal shaker (TGK FNX-220). The amplitude and frequency are 15 mm and 150 rpm, respectively. This oscillation was strong enough to spread paste evenly over the bottom of the container and cause a directional crack pattern after drying.

The paste sample in the container was set on an electric balance (A&D EK-600H), and the entire setup was fixed on the horizontal shaker with four laser displacement sensors (OPTEx-FA CD1-30), as depicted in Fig. 2(b). The springs were bent upward due to the contraction of the paste as it dried, and we measured the vertical displacement,  $w(t)$ , of the free end of each spring with a laser displacement sensor. The springs labeled “A” and “B” in Fig. 2(c) are free to bend along the directions parallel

and perpendicular to the shaking, respectively. In order to average small variations in the drying rate and the response of the springs, we repeated experiments  $K = 2$  or 4 times for a given set of conditions, rotating the container by  $90^\circ$  on the shaker before each experiment, and thereby obtained  $2K$  sets of results for the A and B directions, respectively.

We dried each sample uniformly at room temperature ( $25 - 27^\circ\text{C}$ ) with a humidity of  $20 - 40\%$ , while monitoring the sample's weight. Then, we calculated the mass per unit area of the container bottom,  $m(t)$ , and the solid volume fraction,

$$\phi(t) \equiv \left\{ 1 + \left( \frac{m(t)}{m_{\text{final}}} - 1 \right) \frac{\rho_{\text{CaCO}_3}}{\rho_{\text{H}_2\text{O}}} \right\}^{-1}, \quad (1)$$

where  $\rho_{\text{CaCO}_3} = 2.72\text{g/cm}^3$ ,  $\rho_{\text{H}_2\text{O}} = 0.997\text{g/cm}^3$ , and  $m_{\text{final}}$  is the mass per unit area after drying.

The thickness of the paste sample decreases while the paste dries until the formation of cracks, after which the thickness does not change significantly [11]. For each spring, we measured the thicknesses of a terminally dry sample at three positions with a micrometer and used the average of these measurements as the sample thickness,  $H$ . We obtained  $H = 4.04 \pm 0.18\text{mm}$  for typical experiments with  $m_{\text{final}} = 0.556\text{g/cm}^2$ . The stresses estimated in this paper are nominal stresses, as they are calculated on the basis of this thickness, for simplicity [16].

**Stress estimation.** — A spring bends during the drying process because of both a decrease in the weight of the paste and the emergence of torque exerted by horizontal tensions developing in the paste. The gravitational force changes by  $\Delta m(t)g$  per unit area from the initial state, where  $g$  is the acceleration due to gravity and  $\Delta m(t)$  is the total change in  $m(t)$ . The paste sample has a free top surface, and the length,  $L$ , is much larger than the thicknesses  $h$  and  $H$ . Assuming the paste sample to exist in the interval  $(h/2, H + h/2)$  along the  $z$  axis initially, the horizontal stresses,  $\sigma_{xx}(z, t)$ , in the sample exert a torque

$$\int_{\frac{h}{2}}^{H+\frac{h}{2}} dz z \sigma_{xx}(z, t) \equiv \frac{H(H+h)}{2} \sigma^*(t) \quad (2)$$

on the bottom, where we have defined  $\sigma^*(t)$  so that  $\sigma_{xx}(z, t) = \sigma^*(t)$  for uniform stresses.

For each spring,  $\sigma^*(t)$  can be estimated from  $w(t)$  by using the bending theory of a thin elastic plate, because a stainless steel spring is sufficiently hard compared with the paste for there to exist a neutral plane. From Eqs. (12) and (14) in the appendix, the displacement from the initial state,  $\Delta w \equiv w(t) - w(0)$ , is given by

$$\Delta w = \frac{L^2}{8D_b} \{ 2(H+h)H\sigma^*(t) - L^2\Delta m(t)g \}. \quad (3)$$

Here,  $D_b$  is the bending elastic modulus of a spring. Under conditions with no paste in the container, we measured

the spring constant  $k$  of each spring by applying forces to the free end with a bend-testing machine (Shimadzu AGS-X) and calculated  $D_b$  by using Eq. (13) in the appendix. The measured values differ slightly among the four springs. For example,  $k = 0.51 \pm 0.02\text{N/mm}$  for the  $0.2\text{mm}$ -thick springs, which corresponds to  $\Delta w \simeq 0.5\text{mm}$  for  $\sigma^* = 10\text{kPa}$ .

**Results.** — We found that the stress,  $\sigma^*(t)$ , increases during drying and then decreases at the time of crack formation. The behavior of  $\sigma^*(t)$  is similar for the water-rich and water-poor cases and in the A and B directions. However, we found a slight dependence on the direction, as described below.

Figure 3 depicts  $\sigma^*(t)$  in the water-rich case and those for the A and B directions separately in the water-poor case as a function of  $\phi(t)$ . We carried out two experiments ( $K = 2$ ) in each case using  $0.2\text{ mm}$ -thick springs. The results are plotted as the averages of  $\sigma^*(\phi)$ , with the standard deviations indicated by the gray regions. It is seen that, in the water-poor case, the tensile stress in the A direction drops sooner than that in the B direction, because the paste remembers the direction of the shaking and cracks perpendicular to the direction of the shaking formed first. The stress in the B direction attains a maximum at a larger value of  $\phi$ , as it continues to increase with further drying. The development of stress in the water-rich case, indicated by the dotted line, is similar to that in the A direction in the water-poor case, except that the plot is shifted to the left by  $0.01 - 0.02$  along the  $\phi$  axis. This shift suggests weak hysteresis, as the stresses are not always determined only by  $\phi$  during the drying paste. This is also consistent with the empirical fact that water-rich paste cannot remember the direction of shaking even when it is applied after  $\phi$  increases above the liquid limit during the drying process.

The maximum stress in the water-rich case is approximately the same as that in the A direction in the water-poor case. That is, the stress required for the first crack formation does not depend significantly on whether or not the paste retains memory of the shaking. We also investigated the dependence of the maximum stress on the thickness of the sample (the graph is omitted here) and found that the maximum stress increases as the thickness decreases. This result is consistent with the results of previous studies of the fracture conditions of thin films [17–20].

We next carried out a more precise investigation of stresses, focusing on the stage before crack formation. Figure 4(a) plots the stresses in the A and B directions in the water-poor case. The results appearing here are the averages over four experiments ( $K = 4$ ) for each direction. We found that the stresses along the two directions differ slightly even before that along the A direction reaches its maximum. Similar differences were also found when we altered the thickness of the springs from  $h = 0.2\text{mm}$  to  $0.3\text{mm}$  and  $0.15\text{mm}$  (with  $D_b$  changing by factors of 3.16 and 0.44, respectively). However these differences are

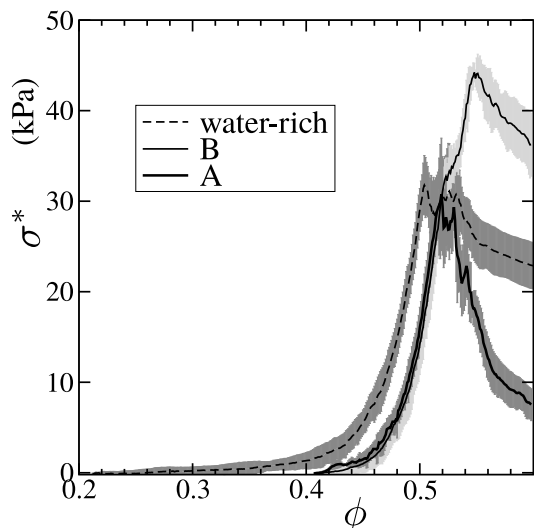


Fig. 3: Development of stress with desiccation.  $\phi$  increases rightward along the horizontal axis, as drying progresses. “A” and “B” indicate the stresses parallel and perpendicular to the direction of shaking, respectively, in the water-poor case. After the formation of the first crack, large differences appear between A and B. The dotted curve represents the stress in the water-rich case.  $m_{\text{final}} = 0.455 \pm 0.01 \text{g/cm}^2$  for the both cases.

much smaller than the stresses themselves and are comparable to the magnitudes of the error bars in this graph. The main cause of errors is inferred to be variation in the response of the springs, which may be ascribable to the slight geometrical differences in the soft lateral walls made by hand. These systematic errors could not be removed completely, even though we calculated Eq. (3) by using  $D_b$  measured for each spring.

Figure 4(b) elucidates the difference between the stresses in the A and B directions,  $\sigma_A^* - \sigma_B^*$ , averaged over the four springs. The method of averaging here is different from that used in Fig. 4(a). In order to obtain  $\sigma_A^* - \sigma_B^*$  for each spring, we first chose four data (two pairs in the A and B directions) that were obtained from the same spring in the four experiments and calculated the difference between the averages of the A and B pairs. The result confirms that the stress anisotropy increases while the sample is drying before crack formation. The difference  $\sigma_A^* - \sigma_B^*$  is positive and approximately  $\sigma_A^*/10$ . The fact that  $\sigma_A^* - \sigma_B^*$  is positive is consistent with both residual tension theories [8–10] and the sign suggested by the bending phenomena in a soft container like that depicted in Fig. 1.

**Discussion.** – Directional crack growth could be caused by anisotropy in either the fracture strength or the amount of elastic energy that can be released, as described by fracture mechanics. We should note that the discrepancy between the maximum values of the stress in the A and B directions in the water-poor case does not always imply anisotropy in the fracture strength. The formation

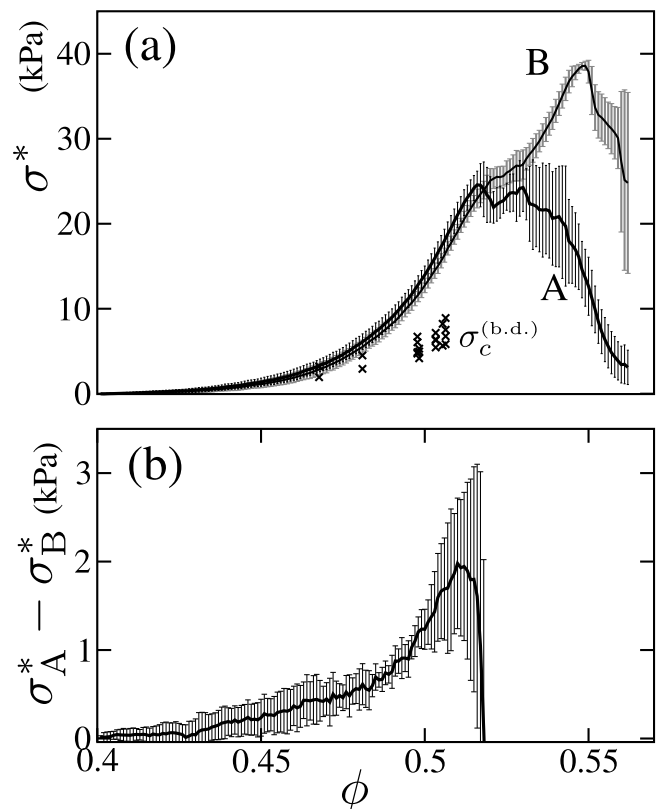


Fig. 4: (a) Evolution of the stress during the drying process of paste in the water-poor case. The data were obtained from four experiments with  $m_{\text{final}} = 0.5564 \pm 0.003 \text{g/cm}^2$ . The symbols “x” indicate the yield stresses,  $\sigma_c^{(b.d.)}$ , obtained from bending-down tests. (b) The difference between  $\sigma_A^*$  and  $\sigma_B^*$ . The data were averaged over the four springs after calculating  $\sigma_A^* - \sigma_B^*$  for each spring. The error bars represent the standard deviations.

of parallel cracks coinciding with the maximum stress in the A direction decreases tension in the direction B and suppresses the formation of cracks parallel to the direction of shaking. As a result, the fracture strength required for subsequent cracking could increase during further desiccation.

The fact that  $\sigma_A^* - \sigma_B^*$  is non-zero even before crack formation suggests that there exists anisotropy in the macroscopic properties of the paste. This difference is small compared with the stresses themselves, but it increases to about 2kPa. As the yield stress of the paste is approximately 5Pa for the initial value of the solid volume fraction [3],  $\sigma_A^* - \sigma_B^*$  increases by a factor of at least several hundred during the drying process. Nonlinear elasticity of the paste would provide a simple explanation if indeed we could regard paste as a nonlinear elastic material. When anisotropy in the plastic strain is induced by the shaking and this anisotropy persists through the drying process, the increase in the rigidity due to dry contraction could cause such amplification. However, as discussed below, the material does not behave as a nonlinear elastic material; on the contrary, as we establish experimentally below, it

remains plastic throughout the drying process.

Because the yield stress of drying paste is too large to be measured with a standard rheometer, we carried out bending tests on paste samples at intermediate stages in the drying process. Figure 5 displays a typical result for the change in the stress,  $\sigma^*$ , as a function of the applied displacement,  $\Delta w$ . The result for both bending-up and bending-down tests carried out on two samples with the same solid volume fraction are merged in this graph. In both tests, we prepared the paste samples in the same manner as in the experiments considered in Fig. 4 and moved the free end of a spring up and down with the bend testing machine (Shimadzu AGS-X). The bending was repeated three times, while changing the speed and the maximum displacement by a factor of 5. From Eqs. (13) and (14) appearing in the appendix, the vertical displacement of the free end of a spring,  $\Delta w(t)$ , is determined by both the applied force,  $F(t)$ , and the change in the horizontal stress,  $\Delta\sigma^*$ , as

$$k\Delta w(t) = \frac{3W(H+h)H}{4L}\Delta\sigma^*(t) + F(t). \quad (4)$$

The quantity  $\Delta\sigma^*(t)$  is calculated by subtracting the measured forces  $F(t)$  from the restoring force of the spring,  $k\Delta w(t)$ . Because  $\Delta w(t)$  is approximately proportional to the change in the bending curvature of the bottom, the paste sample is compressed horizontally for  $\Delta w(t) > 0$  (bending up) and stretched for  $\Delta w(t) < 0$  (bending down). Therefore, this graph roughly represents the stress-strain relation for the paste although the accuracy is not sufficient to determine whether anisotropy exists in the yield stresses or in the elastic moduli of the paste. The graph has no symmetry with respect to the origin. Paste behaves as a typical elasto-plastic material with respect to stretching: It has a constant yield stress,  $\sigma_c^{(b.d.)}$ , while it is rather elastic for very small deformation. On the other hand, paste is always plastic and exhibits hardening under compression. The quantity  $\sigma_c^{(b.d.)}$  is plotted by the symbol “x” in Fig. 4(a). These data were obtained from samples in various states of drying. It is seen that the yield stress increases with drying and that it is less than  $\sigma_A^*$  and  $\sigma_B^*$  but larger than  $\sigma_A^* - \sigma_B^*$ . The results indicate that stresses increasing with drying can readily cause plastic deformation until just before crack formation.

**Conclusion.** – We measured horizontal stresses arising in a paste sample by monitoring the bending of elastic plates and found that stress anisotropy develops during the drying process until crack formation in paste under water-poor conditions that was subject to horizontal shaking at the beginning of the experiment. Our results support the prediction of the residual tension theories regarding the memory effect of shaking. Our bending tests indicate that paste behaves as a plastic material until just before crack formation. We need a theoretical model consistent with these facts to understand how the weak anisotropy induced by shaking results in a directional

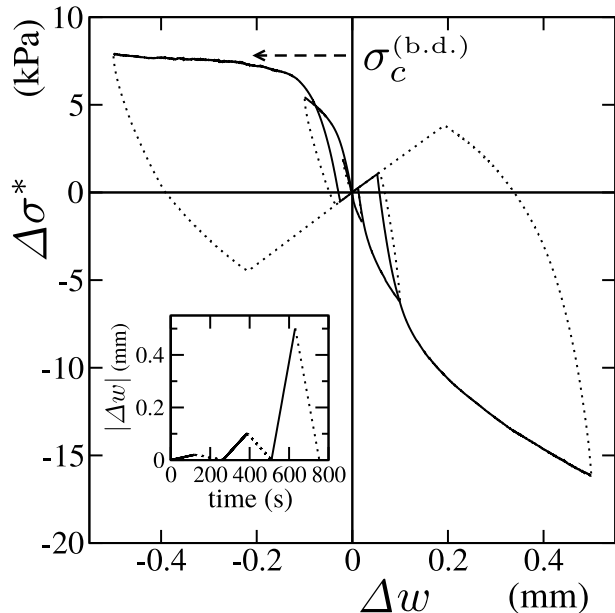


Fig. 5: Stresses caused by bending a spring up and down. Bending-up and bending-down tests were carried out on paste samples in the same drying state with  $0.505 \leq \phi \leq 0.510$  for the water-poor case. The inset shows the protocol of the displacement control in both tests. The dotted lines indicate the return motions. The paste samples were covered to prevent further desiccation during the tests. These tests did not significantly affect the crack patterns, which appeared after drying.

crack pattern.

\*\*\*

The authors acknowledge M. Otsuki, Ooshida Takeshi, T. Mizuguchi, A. Nishimoto and T. Yamaguchi for valuable discussions and advices. This research was supported by Grants-in-Aid for Scientific Research (KAKENHI C 26400395) from JSPS, Japan.

**Appendix.** – A thin elastic plate bends in accordance with the Föppl-von Kármán equations [21]. For a sample in which a uniform sheet of paste of thickness  $H$  is supported by an elastic plate of thickness  $h$ , the basic equations are derived in essentially the same manner. Let us assume that the sample has two free surfaces, at  $z = -h/2$  and  $H + h/2$ , and that its thickness,  $h + H$ , is sufficiently smaller than the length  $L$ :  $\Delta \equiv (h + H)/L \ll 1$ . Because the sample is approximately under the plane stress condition, the stresses are described by Piola-Kirchhoff tensors,  $\sigma_{\alpha\beta}$ , in the horizontal directions  $\alpha, \beta = x, y$ .

The strain tensors in the layer are given by

$$\epsilon_{\alpha\beta} \simeq \frac{1}{2} \left( \frac{\partial u_\beta}{\partial x_\alpha} + \frac{\partial u_\alpha}{\partial x_\beta} + \frac{\partial u_z}{\partial x_\alpha} \frac{\partial u_z}{\partial x_\beta} \right) - z \frac{\partial^2 u_z}{\partial x_\alpha \partial x_\beta}, \quad (5)$$

where  $(u_x, u_y, u_z)$  represents the displacements in the  $xy$  plane. These strain tensors are valid if the variables are

small satisfying  $u_\alpha = O(L\Delta^2)$ ,  $u_z = O(L\Delta)$  and  $\epsilon_{\alpha\beta} = O(\Delta^2)$ .

When an external forces per unit basal area,  $f$ , is applied in the  $z$  direction, requiring the free energy to be minimized with respect to variation in the displacement,  $(\delta u_x, \delta u_y, \delta u_z)$ , yields

$$\int_0^L dx \int_0^W dy \left( \int_{-h/2}^{H+h/2} dz \sigma_{\alpha\beta} \delta \epsilon_{\alpha\beta} - f \delta u_z \right) = 0. \quad (6)$$

From this condition, we obtain the basic equations of force balance in and out of the plane,

$$\frac{\partial \langle \sigma_{\alpha\beta} \rangle}{\partial x_\beta} = 0 \quad (7)$$

and

$$(H+h) \left( \langle \sigma_{\alpha\beta} \rangle \frac{\partial^2 u_z}{\partial x_\alpha \partial x_\beta} + \frac{\partial^2 \langle \sigma_{\alpha\beta} z \rangle}{\partial x_\alpha \partial x_\beta} \right) + f = 0, \quad (8)$$

respectively, and the free boundary conditions,  $n_\beta \langle \sigma_{\alpha\beta} \rangle = n_\beta \langle \sigma_{\alpha\beta} z \rangle = 0$ , and  $n_\beta (\langle \sigma_{\alpha\beta} \rangle \partial u_z / \partial x_\alpha + \partial \langle \sigma_{\alpha\beta} z \rangle / \partial x_\alpha) = 0$ , where  $\langle \cdot \rangle$  denotes the average over the range  $-h/2 \leq z \leq H+h/2$  and  $(n_\beta)$  is the normal vector of the boundary in the  $xy$  plane.

When a sample with a free end at  $x = 0$  bends only along the  $x$  direction,  $u_z(x, t)$  is calculated easily by assuming  $\langle \sigma_{xy} \rangle = 0$  and uniformity in the  $y$  direction. As Eq. (7) gives  $\langle \sigma_{xx} \rangle = 0$ , and therefore the first term in Eq. (8) vanishes, integrating Eq. (8) yields

$$-(H+h) \langle \sigma_{xx} z \rangle = \int_0^x dx' \int_0^{x'} dx'' f \equiv N(x, t). \quad (9)$$

Dividing the average on the left-hand side into two parts, we obtain

$$(H+h) \langle \sigma_{xx} z \rangle = \int_{-h/2}^{h/2} dz \sigma_{xx} z + \int_{h/2}^{H+h/2} dz \sigma_{xx} z \\ \equiv h \langle \sigma_{xx} z \rangle_h + H \langle \sigma_{xx} z \rangle_H. \quad (10)$$

The first term here is proportional to the curvature of the elastic plate,  $\partial^2 u_z / \partial x^2$ . Therefore, we obtain

$$D_b \frac{\partial^2 u_z}{\partial x^2} - H \langle \sigma_{xx} z \rangle_H = N, \quad (11)$$

where the coefficient  $D_b$  is the bending elastic modulus.

Imposing the fixed boundary conditions  $u_z = \partial u_z / \partial x = 0$  at  $x = L$ , the displacement of the free end,  $w(t) \equiv u_z(0, t)$ , can be calculated as the superposition of the contributions from the forces acting on the elastic plate. For gravitational forces  $m(t)g$  acting in the downward direction, we have

$$w(t) = -\frac{L^4}{8D_b} m(t)g, \quad (12)$$

where we have used  $N(x, t) = -\frac{1}{2}m(t)gx^2$ . For an external force  $F(t)$  applied to the free end in the  $z$  direction, we have  $N(x, t) = (F(t)/W)x$ , and thus

$$w(t) = \frac{L^3}{3D_b W} F(t) \equiv \frac{1}{k} F(t), \quad (13)$$

where  $k$  is the spring constant of the linear elastic plate. For uniform stresses  $\sigma_{xx}(x, t) = \sigma^*(t)$  arising in the paste layer ( $h/2 < z < H + h/2$ ), we obtain

$$w(t) = \frac{L^2(H+h)H}{4D_b} \sigma^*(t), \quad (14)$$

since  $\langle \sigma_{xx} z \rangle_H = (H+h)\sigma^*(t)/2$ .

## REFERENCES

- [1] NAKAHARA A. and MATSUO Y., *J. Phys. Soc. Jpn.*, **74** (2005) 1362; *Phys. Rev. E*, **74** (2006) 045102(R); *J. Stat. Mech.*, **2006** (P07016) .
- [2] PAUCHARD L., ELIAS F., BOLTEHAGEN P., CEBERS A. and BACRI J. C., *Phys. Rev. E*, **77** (2008) 021402.
- [3] NAKAHARA A., SHINOHARA Y. and MATSUO Y., *J. Phys. : Conf. Ser.*, **319** (2011) 012014.
- [4] KHATUN T., CHOUDHURY M. D., DUTTA T. and TARAFDAR S., *Physical Review E*, **86** (2012) 016114.
- [5] MATSUO Y. and NAKAHARA A., *J. Phys. Soc. Jpn.*, **81** (2012) 024801.
- [6] NAKAYAMA H., MATSUO Y., OOSHIDA T., and NAKAHARA A., *Eur. Phys. J. E*, **36** (2013) 1.
- [7] GOEHRING L., NAKAHARA A., DUTTA T., KITSUNEZAKI S. and TARAFDAR S., *Desiccation Cracks and their Patterns: Formation and Modelling in Science and Nature in Statistical Physics of Fracture and Breakdown Series* (Wiley) 2015.
- [8] OTSUKI M., *Phys. Rev. E*, **72** (2005) 046115.
- [9] OOSHIDA T., *Phys. Rev. E*, **77** (2008) 061501.
- [10] OOSHIDA T., *J. Phys. Soc. Jpn.*, **78** (2009) 104801.
- [11] KITSUNEZAKI S., *J. Phys. Soc. Jpn.*, **78** (2009) 064801.
- [12] KITSUNEZAKI S., *Phys. Rev. E*, **87** (2013) 052805.
- [13] Figure 1 seems to resemble other buckling phenomena like a grilled dry squid (*surume* in Japanese). However its anisotropy is not inherent, which can be controlled by shaking. See supplemental material at [URL inserted by EPL].
- [14] TIRUMKUDULU M. S. and RUSSEL W. B., *Langmuir*, **21** (2005) 4938.
- [15] PETERSEN C., HELDMANN C. and JOHANNSMANN D., *Langmuir*, **15** (1999) 7745.
- [16] The first crack formation occurs at  $\phi(t) \equiv m_{\text{final}}/(\rho_{\text{CaCO}_3} H) \simeq 0.51 \equiv \phi_c$  approximately. The thickness of a paste sample before the crack formation can be estimated because it is inversely proportional to  $\phi(t)$  when  $\phi(t) < \phi_c$ . However such correction to the stress estimation does not change the main results.
- [17] BEUTH J. L. JR., *Int. J. Solids Structures*, **29** (1992) 1657.
- [18] ROUTH A. F. and RUSSEL W. B., *Langmuir*, **15** (1999) 7762.
- [19] MAN W. and RUSSEL W. B., *Phys. Rev. Lett.*, **100** (2008) 198302.

- [20] SINGH K. B. and TIRUMKUDULU M. S., *Phys. Rev. Lett.*, **98** (2007) 218302.
- [21] AUDOLY B. and POMEAU Y., *Elasticity and Geometry: From hair curls to the non-linear response of shells* (OUP Oxford) 2010.